INNSPUB

International Journal of Biosciences | IJB |
ISSN: 2220-6655 (Print), 2222-5234 (Online)
http://www.innspub.net
Vol. 10, No. 3, p. 406-417, 2017

RESEARCH PAPER OPEN ACCESS

Development of ultrasensitive biological immunoassay system using Fe_3O_4 nanoparticles and magnetic sensor in the liquid phase

Md. Anwarul Kabir Bhuiya[1*], Raihana Ferdaws[1], Masaki Asai[2], Yuichi Higuchi[2] Takeshi Yoshida[2], Keiji Enpuku[2], Edmund Soji Otabe[3]

[1]*Department of Materials Science and Engineering, University of Rajshahi, Rajshahi, Bangladesh*

[2]*Department of Electrical and Electronic Engineering, Kyushu University, Fukuoka 819-0395, Japan*

[3]*Computer Science and Electronics, Kyushu Institute of Technology, Iizuka, Japan*

Key words: Bio-nanotechnology, MR sensor, Fluxgate sensor, Brownian Relaxation, AC Susceptibility, Nanoparticles.

http://dx.doi.org/10.12692/ijb/10.3.406-417 Article published on March 31, 2017

Abstract

In this paper, we first describe details of the measurement system (MR and Flux Gate sensor). The measurement system using the MR sensor showed a sensitivity to detect 1.4×10^7 of the markers in 60 µl of solution. The sensitivity was improved as 8.3×10^6 when the flux gate sensor was used. The sensitivity of the present method was estimated as 3.8×10^{-16} and 2.3×10^{-16} mol/ml in terms of the molecular-number concentration for the MR and the flux gate sensor, respectively. We next demonstrate the detection of biological targets known as biotins, which were conjugated on the surface of the polystyrene beads with a diameter of 3.3 µm. The minimum detectable number of beads was N_p = 10,000 and 5,000 for the case of the MR and the flux gate sensor, respectively. Since about 700 biotins were fixed on the single polymer bead, the minimum detectable number of biotins was estimated as $N_b = 7 \times 10^6$ and 3.5×10^6 for the case of the MR and the flux gate senor, respectively. A strong relationship was obtained between the number of bound markers and the number of biotin-conjugated polymer beads, which confirmed the validity of the method. The detection sensitivity can be estimated as 1.9×10^{-16} and 0.8×10^{-16} mol/ml in terms of the molecular-number concentration of biotin for the MR and the flux gate sensor, respectively. These results are consistent with the estimated sensitivity of the measurement system.

* **Corresponding Author:** Md. Anwarul Kabir Bhuiya ✉ mkabir@ru.ac.bd

Introduction

Magnetic markers, which are composed of polymer-coated magnetic nanoparticles, have been extensively studied for use in biological applications such as cell separation, immunoassays, hyperthermia, and drug delivery. Immunoassays are used to detect biological targets such as disease-related proteins and cells. Magnetic immunoassay techniques that utilize magnetic markers have recently been developed. One of the advantages of this magnetic method is that we can perform immunoassays in the liquid phase; that is, we can magnetically distinguish bound markers from unbound (free) markers. This function can be utilized to eliminate the time-consuming washing process used to separate the two types of markers, i.e., the so-called bound/free separation [1, 2, 3].

Experimental

Sensors

MR (Magneto Resistive) Sensor

In our experiment, we used the Honeywell MR sensor for the measurement. It is very necessary to learn the details literature of the sensing device. We also use Flux Gate sensor as well. The Honeywell HMC100x and HMC102x magnetic sensors are one and two-axis surface mount sensors designed for low field magnetic sensing. By adding supporting signal processing, cost effective magnetometers or compassing solutions are enabled. These small, low cost solutions are easy to assemble for high volume OEM designs. Applications for the HMC100x and HMC102x sensors include Compassing, Navigation Systems, Magnetometry, and Current Sensing. The HMC100x and HMC102x sensors utilize Honeywell's Anisotropic Magnetoresistive (AMR) technology that provides advantages over coil based magnetic sensors [6, 9]. They are extremely sensitive, low field, solid-state magnetic sensors designed to measure direction and magnitude of Earth's magnetic fields, from tens of micro-gauss to 6 gauss. Honeywell's Magnetic Sensors are among the most sensitive and reliable low-field sensors in the industry. The Honeywell HMC100x and HMC102x Anisotropic Magneto-Resistive (AMR) sensors are simple resistive Wheatstone bridges to measure magnetic fields and only require a supply voltage for the measurement. With power supply applied to the bridges, the sensors convert any incident magnetic field in the sensitive axis directions to a differential voltage outputs [19].

Flux gate sensor

This section describes the features common to the Bartington Flux Gate Sensor System which is used in our experiment. Three fluxgate sensing elements are mounted orthogonally at one end of an enclosure which also contains the electronic circuitry. The connector is mounted at the opposite end of the enclosure. The position and direction of each sensing element is shown on the outside of the sensor, together with the product code, measuring range and serial number.

The sensors require a power supply of between ±12V and ±17V and provide three high precision analog outputs of 0 to ±10V full scale, proportional to the magnetic field along each axis. For a unit with a full scale range of ±100μT the output voltage for each axis is 0.1V/μT of the field in the direction of that axis. The relationship between the magnetic field and the analog output is linear and the frequency response is maximally flat from d.c. to 1 kHz with a bandwidth of 3 kHz [18, 19].

Information extraction

As described previously, the signal in the pick-up coil depends not only on the external field, but also on the excitation field and heterogeneity of the magnetic cores. To extract the relevant information about the external field from the signal generated in the pickup-coil a number of techniques has been developed.

Time domain detection

Using the single core setup the field strength can be calculated from the distance (in the time domain) between voltage peaks on the pick-up signal. The resolution of this method is limited by the temporal resolution of the counter measuring the distance between the peaks. Since counters and many fast digital signals are needed much noise are generated and limits this setup as well.

Second harmonic

The second harmonic of the pick-up signal contains much of the information about the magnetic field and has frequently been used in analogue magnetometers. The second harmonic is detected using a phase detector. However the since the pick-up coil is only decoupled from the excitation coil to a certain degree in real magnetometers, feed through of large components of the fundamental and the odd higher harmonics have to be suppressed. By applying a band pass filter this feed through is filtered out and the second harmonic will remain [4].

Correlation

By correlating the signal from the pick-up coil of the magnetometer with a reference signal all samples from the pick-up coil can be used to measure the magnetic field. The correlation signal is constructed using measurements of the response to a magnetic field in two opposite directions. This reference signal contains even harmonics of the excitation frequency. Correlation over one excitation period removes all odd harmonics, and is equivalent to a matched filtering of the pick-up signal [4].

The geometry of the ferromagnetic core of the fluxgate magnetometer affects the sensitivity of the device. This is mainly caused by the demagnetization factor (D) being heavily dependent on core geometry. The most common geometries are rod, double rod, ring and race track. Rod magnetometers are described above and are a very well tested design. The ring core design was first used 1928 and is very well tested [4].

Sensing System

Figure 1, illustrates the measurement system. A disk-shaped sample plate, which has 12 reaction wells, was used. The well was 5 mm in diameter, and the sample (bound and free markers) was diluted in 60 µl of pure water. The detection of the bound markers was performed by the following three steps. (1) First, an excitation field B_{ex}=40 mT was applied to the sample to align the magnetic moments m of both the bound and the free markers. (2) Then, the sample plate was rotated by an (3) After T = 1.5 s, the reaction well comes above the magnetic sensor. The MR and the

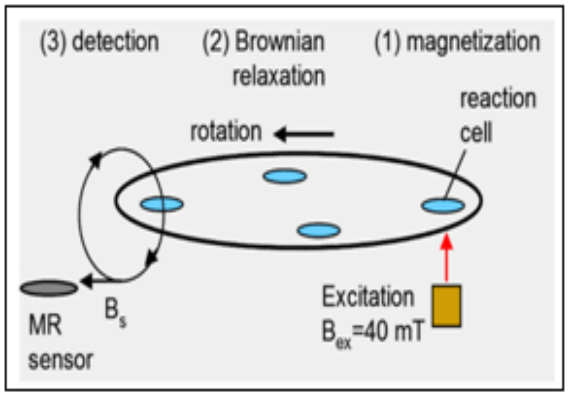

Fig. 1. Detection system using relaxation measurement. (Honeywell MR System used).

Flux gate sensors were installed 2 mm and 4 mm under the sample plate, respectively. A signal field B_s, which was produced by the circular flux due to M of the bound markers, was detected.

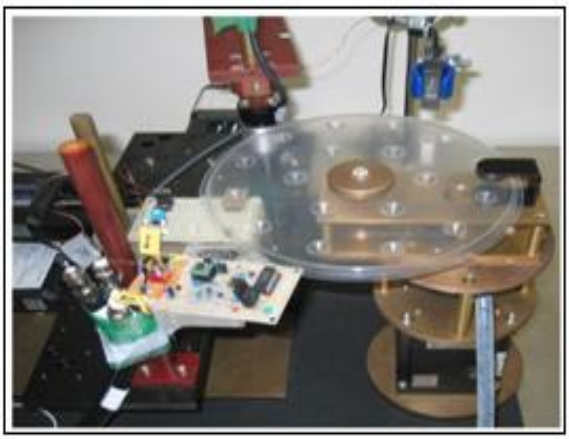

Fig. 2. Laboratory Setup.

For the magnetic sensors, we used a commercial MR sensor (HMC1001, Honeywell, USA) and a Flux gate sensor (Bartington, UK). Here, the MR sensor consisted of a resistive bridge made by 4 thin films, which were arranged in an area of 1 mm × 1 mm. The nominal sensitivity of the MR and flux gate sensors was 160V/T and 14.3×10^6 V/T, respectively.

The sensitive axis of the MR and flux gate sensors was set to a direction parallel to the sample plate, and the signal field B_s was measured, as shown in Figure 1.

Figure 3, shows and waveform of the detected signal when the sample plate was rotated at a speed of 20

rpm. In each reaction well, markers with different weights were set, and the excitation field Bex = 40 mT was applied, as shown in Figure 1. In this experiment, dried markers were used to simulate the bound markers. As shown in Figure 3. (a), we obtained the signal when the sample passed above the MR sensor. The amplitude of the signal decreased with the decrease in the weight of the markers. Similar result was obtained when we used the flux gate sensor, as shown in Figure 3. (b).

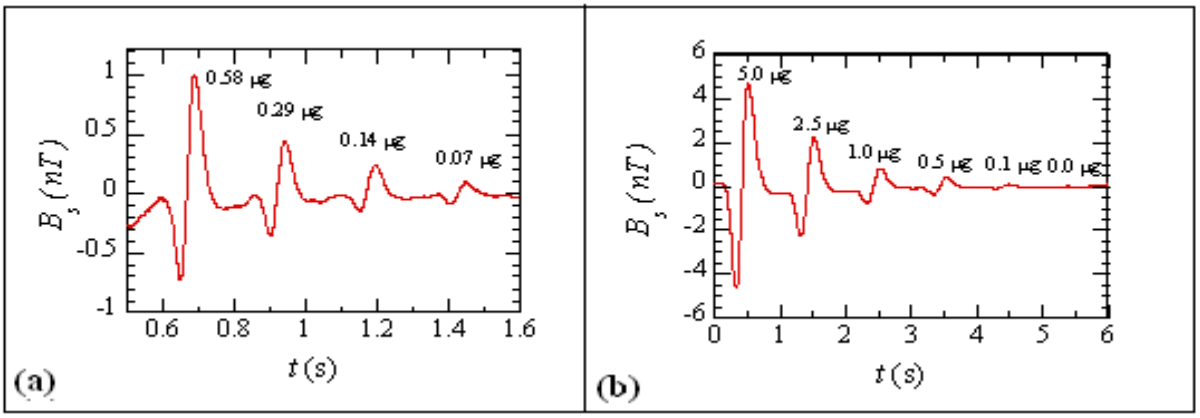

Fig. 3. Waveform of the detected signal when the sample plate was rotated. (a) Signal detected with the MR sensor, and (b) signal detected with the flux gate sensor. A marker, whose weight ranged from 0.1 to 5 μg, was set in each well on the plate.

We discuss the sensitivity of the present system. As can be seen from Figure 3. (a), the frequency components of the detected signal existed mainly around f = 8 Hz in the present experimental setup. Therefore, the output of the MR sensor was band-pass filtered between 2 and 16 Hz. The measurement was performed 40 times, and the data was averaged to decrease the system noise.

In this case, the measured peak-to-peak noise of the MR sensor system was 90 pT. Therefore, we could measure a signal field B_s larger than 90 pT.

In the case of the flux gate sensor, on the other hand, the measured peak-to-peak noise was 30 pT. Therefore, the noise of the flux gate sensor was about 1/3 of that of the MR sensor [20].

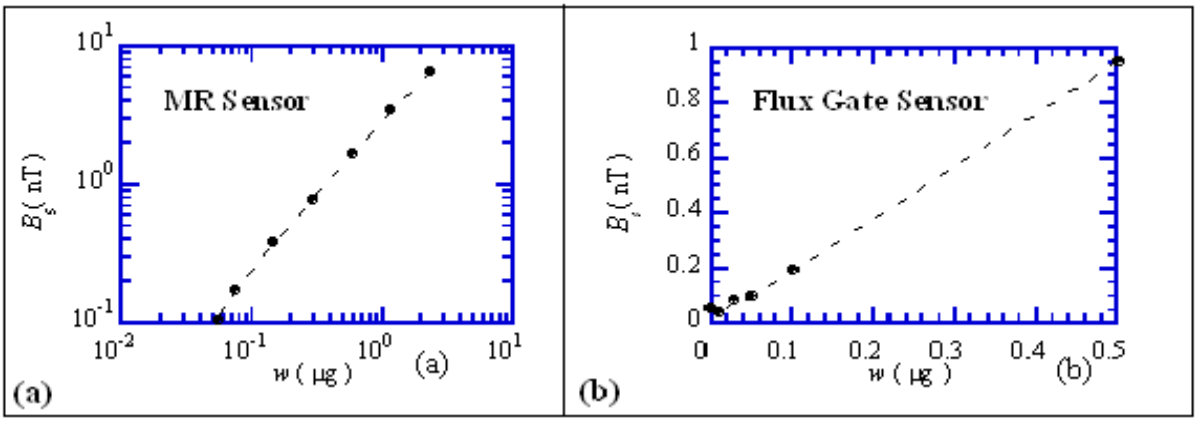

Fig. 4. Relationship between the detected signal B_s and the weight w of the marker. An excitation field B_{ex} = 40 mT was applied. (a) Result obtained with the MR sensor (HMC 1001), and (b) flux gate sensor (Mag-03).

System Sensitivity

We first studied the relationship between the detected signal B_s and the weight w of the bound markers. In the experiment, we used the dried markers in order to simulate the bound markers. The experimental results are shown in Figure 4. The results for the MR

and the flux gate sensors are shown in Figure 4. (a) and 4.(b), respectively.

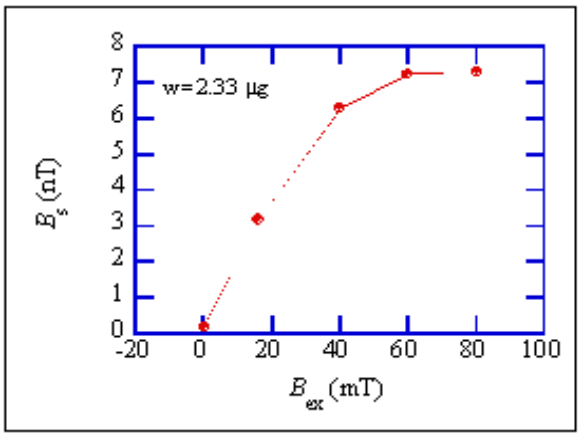

Fig. 5. Relationship between the signal field B_s and the excitation field B_{ex}. The sample was 2.33 μg of magnetic markers (MagCellect particles, R&D Systems, U.S.A.).

As shown, a linear relationship was obtained between B_s and w. The minimum detectable weight of the marker was 50 ng and 30 ng for the case of the MR and the flux gate sensors, respectively. The difference in the susceptibility between them [15].

We note that the signal field B_s detected with the flux gate sensor was smaller than that of the MR sensor, as can be seen from Figure 4. This was because the distance between the flux gate sensor and the sample was larger than the case of the MR sensor; the distance was 4 mm and 2 mm in the case of the flux gate and the MR sensor, respectively. Due to the long distance, the signal from the magnetic marker decays at the sensor position.

Because the mean diameter of the marker was d_h = 110 nm, we can estimate the weight of the single marker as can estimate the weight of the single marker as $w_1 = 3.6 \times 10^{-15}$ g, where we used the specific gravity of Fe_3O_4 as 5.2. Therefore, we can estimate that 50 ng corresponds to the $N_m = 1.4 \times 10^7$ markers. This means that we can expect to detect $N = 1.4 \times 10^7$ biological targets using the MR sensor if we assume that a single marker is bound to a single target. Because the volume of the sample was 60 μl as shown later, this sensitivity can be expressed as 3.8×10^{-16} mol/ml (or 0.38 fmol/ml) in terms of the molecular-number concentration. In the case of the flux gate sensor, minimum detectable weight was 30 ng. Therefore, we can expect the sensitivity of 0.23 fmol/ml in terms of the molecular-number concentration. [20].

We also studied the relationship between the signal field B_s from the bound markers and the value of the excitation field B_{ex}. In this experiment, dried markers were used to simulate the bound markers. The result is shown in Figure 5. As shown, the signal B_s was almost zero when B_{ex} = 0. The value of B_s increased with B_{ex} and reached saturation above B_{ex} > 40 mT. We note that a large field B_{ex} is necessary to align the moment m of the bound markers. This is because the moment m of the bound markers must rotate inside the particle. In the following experiment, therefore, we set the excitation field to B_{ex} = 40 mT. [20].

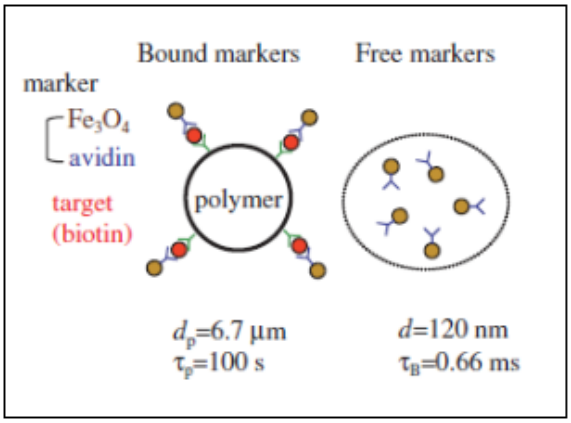

Fig. 6. The markers are bound to the biological targets that are fixed on the surface of large polymer beads. Bound markers are distinguished from the free markers by using.

Measurement system

Detection of biotin

In this section, we will discuss about the detection of number of polymer beads, detection of markers and the biotins. In biochemistry, biotinylation is the process of covalently attaching biotin to a protein, nucleic acid or other molecule. Biotinylation is rapid, specific and is unlikely to perturb the natural function of the molecule due to the small size of biotin. Biotin binds to streptavidin and avidin with an extremely high affinity, fast on-rate, and high specificity, and these interactions are exploited in many areas of

biotechnology to isolate biotinylated molecules of interest. Biotin-binding to streptavidin and avidin is resistant to extremes of heat, pH and proteolysis, making capture of biotinylated molecules possible in a wide variety of environments. There are two measurement techniques of detection of biotin conjugated polymer beads with avidin coated magnetic marker, 1) Brownian relaxation 2) Susceptibility measurement. In our report, we did both types.

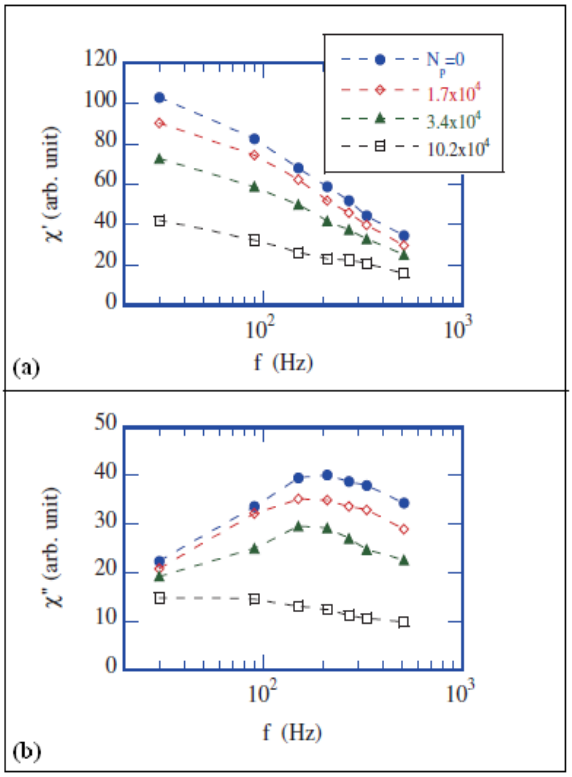

Fig. 7. Frequency dependence of the susceptibility of the magnetic marker in solution. (a) and (b) show the change of the real (χ') and imaginary (χ'') parts, respectively, when the magnetic markers coupled to the polymer beads with different number N_p.

Susceptibility measurement

In this section firstly, we show a method to perform the liquid phase immunoassay using ac susceptibility measurement. In the present method, the bound markers are fixed to large polymer beads, so that the Brownian relaxation time of the bound markers becomes much longer than that of the free markers. This difference can be detected by the change of the ac susceptibility. As an example, we show a detection of biotin-conjugated polymer beads with avidin-coated Fe_3O_4 marker. Changes of the susceptibility caused by the binding reaction between them are shown.

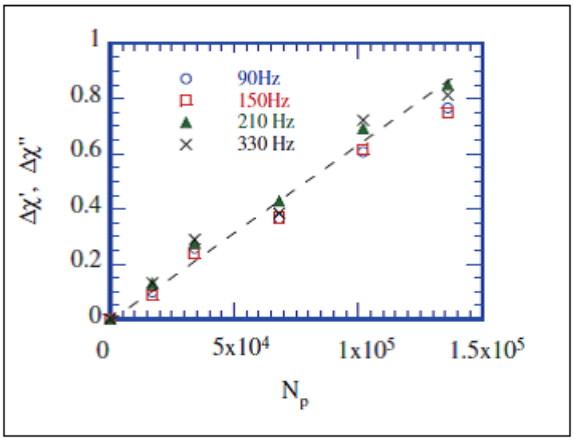

Fig. 8. Relationship between the decrease of the susceptibility and the number N_p of polymer beads. The values of $\Delta\chi'$ measured at f = 90 and 150 Hz, and the values of $\Delta\chi''$ measured at f = 210 and 330 Hz are shown. The broken line is for eyes.

In Figure 6, principle of the detection is schematically shown. As shown, polystyrene particle, whose diameter d_p = 6.7 μm is much larger than that of the magnetic marker, was used to fix the biological targets. After fixing the targets, the markers are put into sample solution. Then, some of the markers are bound to the targets, while others remain unbound (free). The bound markers can be distinguished from the free ones by using the difference in their frequency dependence of the susceptibility, as shown below. When the susceptibility of the magnetic markers is dominated by their Brownian rotation, the real and imaginary part of the susceptibility is given by

$$\chi'(\omega) = \frac{\chi_1}{1+(\omega\tau_B)^2} + \chi_\infty \quad (1)$$

$$\chi''(\omega) = \frac{\chi_1 \omega\tau_B}{1+(\omega\tau_B)^2} \quad (2)$$

With,

$$\tau_B = \frac{3\eta V}{k_B T} \quad (3)$$

where, τ_B is the Brownian relaxation time, $V = \left(\frac{\pi}{6}\right)d^3$ is the volume, d is the diameter, and η is the viscosity of the carrier liquid. In Eq. (4.7), χ_∞ represents the susceptibility at high frequency limit.

As shown in Eqs. (2) and (3), frequency dependence of the susceptibility is determined by the relaxation time τ_B. We define the cut-off frequency by $f = f_c = \frac{1}{(2\pi\tau_B)}$. The real part χ' decreases monotonically with f, while the imaginary part χ'' has a peak value at $f = f_c$. Both values become very small for $f \gg f_c$. [15].

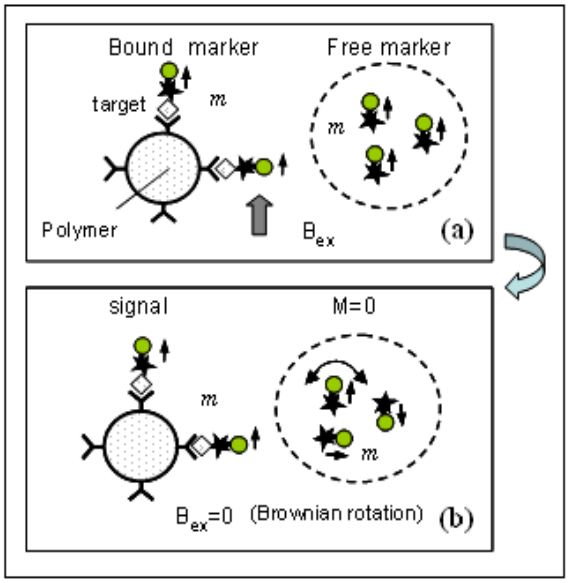

Fig. 9. Principle of liquid-phase immunoassay using the Brownian relaxation of magnetic markers in solution for the detection of biotin conjugated polymer beads. (a) In the case when B_{ex} is applied, and (b) when B_{ex}=0.

In this section, firstly we will discuss about the experimental results where avidin-coated Fe_3O_4 markers (R&D Systems) were used for the experiment. From transmission electron microscope measurement, diameter of each Fe_3O_4 particle was typically 20 – 25 nm. Mean diameter of the marker was obtained as d = 120 nm from dynamic light scattering measurement, which indicates aggregation of Fe_3O_4 particles in making magnetic markers, the relaxation time of the free markers can be calculated from eq. (8) as τ_B= 0.66 ms with d = 120 nm and $\eta = 1\ X\ 10^{-3}$ Pa. s. On the other hand, the bound markers are fixed to the large polymer beads with diameter of d_p = 6.7 m. In this case, Brownian relaxation time of the bound markers is determined by that of the polymer bead, and is given by $\tau_p = \frac{3\eta\left(\frac{\pi}{6}\right)d_p^3}{k_B T}$ = 100 s. This relaxation time is much longer than the value of τ_B= 0.66 ms of the free markers. The cut-off frequencies of the bound and free markers can be calculated as $fc = \frac{1}{(2\pi\tau_B)} = 1.5$ mHz and $fc = \frac{1}{(2\pi\tau_B)} = 240$ Hz, , respectively. Therefore, if we measure the susceptibility in the frequency range 1.5 mHz $\ll$ f $\leq$240 Hz, susceptibility signal from the free markers can be obtained, but the signal from the bound markers becomes almost zero as can be seen from eqs. (6) and (7). This means that the susceptibility of the sample decreases when the binding reaction occurs between the biological targets and the markers. [20].

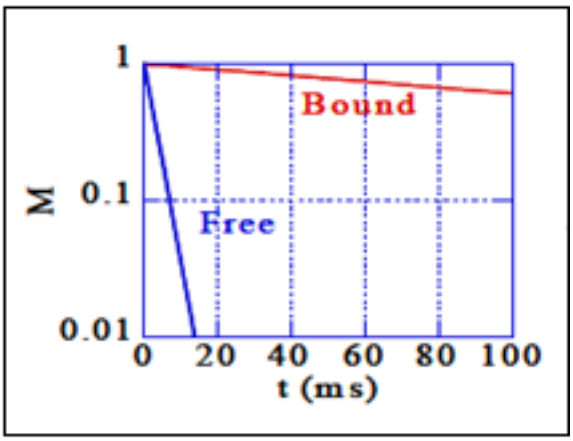

Fig. 10. Decrease of magnetic signal due to the Brownian relaxation. Signal from the free markers decays much faster than that from the bound markers.

We note that, in the above explanation, all markers are assumed to have the same diameter for simplicity. In practical markers, however, distribution of the marker size exists. In this case, eqs. (1) and (2) should be modified so as to take account of the size distribution [8, 9]. In Figure 7. experimental results on the frequency dependence of the susceptibility are shown. Real and imaginary parts of the susceptibility are shown in Figure 7. (a) and Figure 7.(b), respectively. In the experiment, we used biotins as the biological targets, i.e., biotin-conjugated polystyrene particle (Spherotech) was used.

The polymer beads with different number Np and 1.5 μg of avidin-coated magnetic markers were put into 60 l of 10 mM phosphate buffer (pH = 7.4) solution.

After 30 min reaction time, some of the markers coupled the biological target, while others remain unbound, as shown in Figure 6 [18].

Susceptibility of this sample was measured with an MR sensor (Honeywell HMC1001) by applying an external ac field of $\mu_0 H$=300 μT. The vertical axis of Figure 7. Represents the signal voltage from the MR sensor with amplifier gain of 10^5 in unit of mV, where sensitivity of the sensor was 160 V/T. The experimental set up was similar to that reported in ref. 10. Briefly, this sensor has magnetic-field sensitivity in one direction. In order to avoid unwanted coupling between the external field and the sensor, the external filed was applied in the insensitive direction of the sensor. On the other hand, the component of the signal field in the sensitive direction of the sensor was detected. The distance between the sample and the sensor was roughly 1 mm.

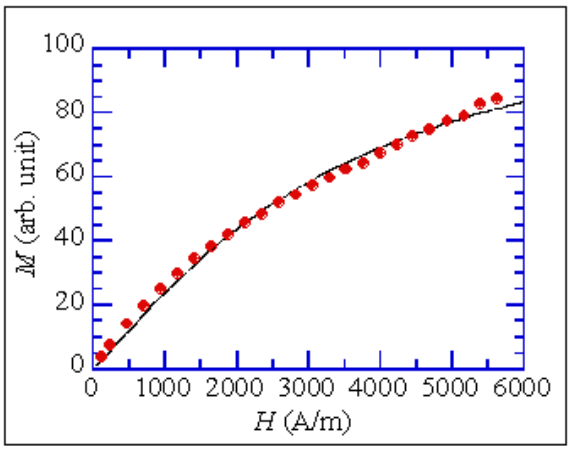

Fig. 11. *M-H* curve of the magnetic markers diluted in pure water.

In Figure 7. (a) and Figure 7. (b), experimental results for the case of N_p = 0 show the susceptibility of the free markers. As shown, real part χ' decreased monotonically with the frequency. On the other hand, the imaginary part χ'' had a broad peak around f = 210 Hz, which is in reasonable agreement with the calculated cut-off frequency $fc = \frac{1}{(2\pi\tau_B)} = 240$ Hz, of the free markers.

As shown in Figure 7. (a) and 7. (b), susceptibility decreased with the number N_p of the polymer beads. This reduction corresponds to the amount of the markers that bound to the polymer beads. Therefore, we studied the relationship between the reduction of the susceptibility and the number N_p.

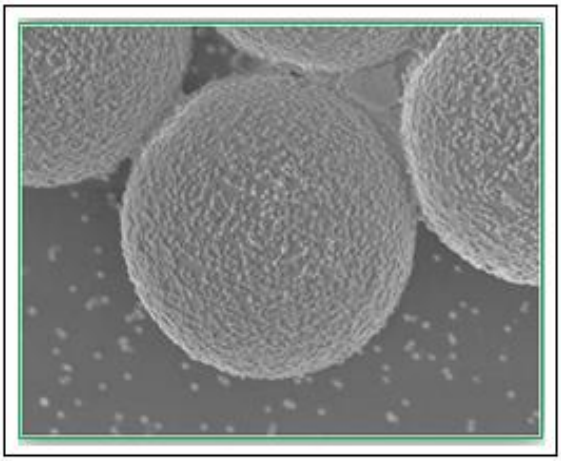

Fig. 12. SEM image of the polymer beads after the binding reaction. Magnetic markers were bound on surface of the polymer bead.

In Figure 8, reductions of the susceptibility defined by $\Delta\chi' = [\chi'(N_p = 0) - \chi'(N_p)]/\chi'(N_p = 0)$ and $\Delta\chi'' = [\chi''(N_p = 0) - \chi''(N_p)]/\chi''(N_p = 0)$ are shown. The values of $\Delta\chi'$ measured at f = 90 and 150 Hz, and the values of $\Delta\chi''$ measured at f = 210 and 330 Hz are shown. As shown, both χ' and $\Delta\chi''$ increased almost linearly with N_p. These results indicate that the liquid phase immunoassay was performed correctly.

We roughly discuss the sensitivity of the present method. From the voltage noise of the MR sensor $S_V^{1/2}$ = 4.5 nV / $Hz^{1/2}$, the measurement bandwidth f = 2 Hz and the amplifier gain $G = 10^5$, we can obtain the peak-to- peak value of the noise voltage as $V_{np} = 2\sqrt{2}\sqrt{\sqrt{S_V \Delta f}}\, G$ = 1.8 mV. As shown in Figure 7. (a), we obtained the signal voltage (χ') of 85 mV at f = 90 Hz for 1.5 μg of marker. Therefore, minimum detectable weight of the marker is expected as 1.5 x (1.8/85) = 0.03 μg. Experimentally, we could detect 50 ng of the marker, which reasonably agrees with the estimated one. Using the mean diameter d =120 nm, we can estimate the weight of the single marker as w = 4.7 x 10^{-15} g, where we used the specific gravity of Fe_3O_4 as 5.2. Therefore, we can estimate that 50 ng corresponds to the number $N_m = 10^7$ of the marker. This means that we can expect to detect N = 10^7

biological targets existing in 60 μl solution, since the single marker bounds to the single target. This sensitivity can be expressed as 3 x 10^{-16} mol/ml (or 0.3 fmol/ml) in terms of molecular-number concentration. [20].

We note that the sensitivity can be improved by increasing the excitation filed *H*, since the signal from the marker is proportional to *H*. We also discuss the dynamic range of the detection. It depends on how precisely we can measure the change of the susceptibility. Since we can easily measure the change from 1 to 100%, dynamic range of 10^2 will be easily obtained. However, it will be difficult to realize very large dynamic range such as 10^4. Therefore, concentration of markers should be chosen corresponding to the number of biological targets to be detected. Finally, we mention the effect of the buffer solution on the aggregation of free markers. In the present experiment, we used 10 mM phosphate buffer (PB) solution, which has been used to detect biological targets such as protein and fungi. In this case, aggregation of the markers was negligible. On the other hand, we observed aggregation of the markers in the phosphate buffer saline (PBS) solution, which consists of 10 mM PB and 150 mM NaCl solution. It is well known that the aggregation is caused by NaCl. Since the PBS solution is necessary to detect cells, it is desired to develop the markers that can avoid aggregation in this solution.

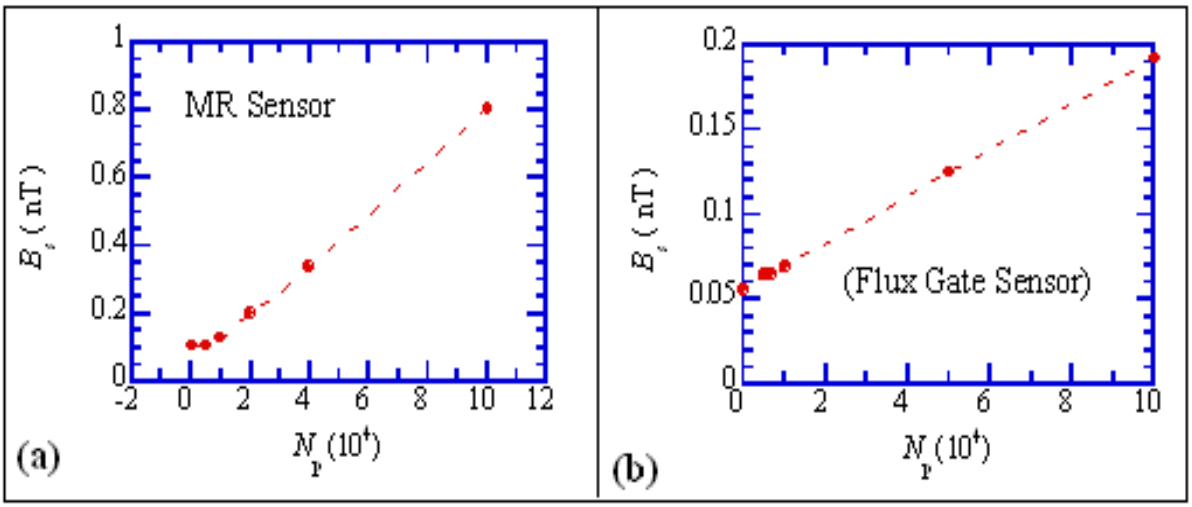

Fig. 13. Relationship between the detected signal Bs and the number of biotin-conjugated polymer beads Np. (a) Result obtained with the MR sensor, and (b) flux gate sensor.

Brownian relaxation measurement method

In this method, Brownian relaxation of magnetic markers in solution was used to perform the liquid-phase detection. Biological targets were fixed on the surface of large polymer beads whose size was typically a few μm. When the magnetic markers were bound to the targets, their Brownian relaxation time was dominated by that of the polymer bead, becoming much longer than that of unbound (free) markers. The resulting difference between the magnetic properties of the bound and free markers was detected by relaxation measurements. Therefore, we can magnetically distinguish between the bound and free markers, i.e., we can omit a time consuming washing process called bound/free separation. We developed a detection system using magneto-resistive (MR) and flux gate sensors.

In order to perform the liquid-phase immunoassay, we used a magnetic marker whose Neel relaxation time is much longer than its Brownian relaxation time. Figure 9. Shows a schematic of the detection principle of the liquid-phase immunoassay.

As shown, we used a large polymer bead to fix the biological targets. When the markers are added, some of the markers are coupled to the targets, whereas others remain uncoupled. The former and the latter

are called bound and free markers, respectively. These bound and free markers coexist in the solution. The bound and free markers can be magnetically distinguished by using the difference in their Brownian relaxation time, as shown below. When an external field Bex is applied to the sample, as shown in Figure 9. (a), the magnetic moments *m* of both the bound and free markers are aligned with the direction of B_{ex}. Then, the excitation field is set to zero. In this case, Brownian rotation of the markers occurs, as shown in Figure 9. (b).

Due to the Brownian rotation, the directions of the magnetic moments start to become random. As a result, the magnetization *M* of the assembly of the markers decays with time as

$$M(t) = M_0 \exp(-\frac{t}{\tau}) \quad (4)$$

Figure 10. shows the calculated results of the Brownian relaxation of both the free and bound markers. When we use a marker with a diameter d_h = 110 nm, the relaxation time of the free marker becomes τ_F = 0.5 ms. Therefore, free markers show rapid relaxation, as shown in Figure 10.. On the other hand, the Brownian relaxation of the bound markers is dominated by the volume of the polymer beads. If we use a polymer bead with a diameter of d_h = 3.3 μm, the relaxation time of the bound markers becomes τ_B = 10 s. Therefore, the bound markers show very slow relaxation compared to the free markers. This means that the signal from the bound markers continues for much longer time, compared to that from the free markers.

We measure the signal from the sample at time *T* after the excitation field was set to B_{ex} = 0. The time *T* is chosen so as to satisfy the condition $\tau_F \ll T \ll \tau_B$ e.g., *T* = 1 s. At this time, the Brownian relaxation of the free markers will be completed, and the signal *M* from the free markers becomes zero, as shown in Figure 9. (b). On the other hand, the signal from the bound markers continues. Therefore, we can detect the signal only from the bound markers; that is, we can magnetically distinguish the bound markers from the free ones.

In the part of the experiment, commercial magnetic markers made of Fe_3O_4 nanoparticles were used (MagCellect particles, R&D Systems, U.S.A.). The size of single Fe_3O_4 particles was measured by transmission electron microscopy and found to be typically 20–25 nm. On the other hand, the size of the marker in pure water was measured by means of dynamic light scattering and found to be typically 110 nm.

Because the single Fe_3O_4 particle size was typically 20–25 nm, it follows that the aggregation of Fe_3O_4 particles occurred in the making of the magnetic markers; that is, the markers consisted of aggregated Fe_3O_4 particles. The magnetic moment *m* of the marker was estimated from the *M-H* curve. In Figure 11, the *M-H* curve of the markers that were diluted in solution is shown.

The circles are the experimental results, whereas the solid line was calculated with the Langevin function $L(\xi) = \coth(\xi) - 1/\xi$ Here, $\xi = mH/k_BT$, and *m* is the magnetic moment of the marker. In the calculation, the value of *m* was taken as an adjustable parameter and was determined as $m = 4.85 \times 10^{-24}$ Wbm so as to obtain the best fit between the experimental results and the calculations.

Now we performed the detection of biological targets called biotins. In the experiment, we used biotins that were conjugated on the surface of polystyrene beads with a diameter of d_p = 3.3 μm (Spherotech Inc, USA). N_p biotin-conjugated polymer beads and 2.33 μg of avidin-coated magnetic markers (MagCellect particles, R&D Systems, U.S.A.) were added to 60 μl of 10 mM phosphate buffer (pH = 7.4) solution. They were incubated for 20 min to complete the binding reaction; the magnetic markers coupled with the polymer beads through the binding reaction between avidin and biotin.

Figure 12. shows the scanning electron microscope (SEM) image of the polymer beads after the binding reaction between biotin and avidin was completed. We can see that the magnetic markers were uniformly

bound on the surface of the polymer beads.

Figure 13. Shows the detected signal B_s when the number of polymer beads N_p was changed. The results for the MR and the flux gate sensors are shown in Figs. 4.20 (a) and 4.20 (b), respectively. As shown, the signal increased almost linearly with the change of the number of polymer beads.

The minimum detectable number of beads was N_p = 10,000 and 5,000 for the case of the MR and the flux gate sensor, respectively. Since about 700 biotins were fixed on the single polymer bead, the minimum detectable number of biotins was estimated as $N_b = 7 \times 10^6$ and 3.5×10^6 for the case of the MR and the flux gate senor, respectively.

The detection sensitivity can be estimated as 1.9×10^{-16} and 0.8×10^{-16} mol/ml in terms of the molecular-number concentration of biotin for the MR and the flux gate sensor, respectively. These results are consistent with those obtained from Figure 4.

Conclusions

We applied the ac susceptibility measurement of the magnetic marker in solution to the liquid phase immunoassay. We detected the biotin-conjugated polymer beads with the avidin-coated Fe_3O_4 markers.

The binding reaction between them was detected by the decrease of the ac susceptibility. Good relationship between the decrease of the susceptibility and the number of the polymer beads confirms the validity of the present method.

Although sensitivity of the present system can be estimated as 3 x 10^{-16} mol/ml in terms of the molecular concentration, much improvement can be expected.

Acknowledgement

This research work has been done with the financial support of MEXT, JAPAN under RISS Lab Kyushu University, Fukuoka, Japan. The researchers also acknowledge the supports of University of Rajshahi and Superconductor Lab, Department of Physics and Information Technology, Faculty of Computer Science and Systems Engineering, Kyushu Institute of Technology, Iizuka, Fukuoka, 820-8502 Japan.

Declaration

All the authors do not have any possible conflicts of interest.

References

1. G. Li, S. Sun, R. J. Wilson, R. L. White, Nader Pourmand and S. X.Wang, Sens. Actuators A 126, 98 (2006).
2. G. Li, S. X. Wang and S. Sun, IEEE Trans. Magn. 40, 3000 (2004).
3. S. X. Wang, S.-Y. Bae, G. Li, S. Sun, R. L. White, J. T. Kemp and C. D. Webb, J. Magn. Magn. Mater. 293 731.
4. Manual of Magnetoresistive and Fluxgate sensor.
5. J. Schotter, P. B. Kamp, A. Becker, A. Puhler, D. Brinkmann, W. Schepper, H. Bruckl and G. Reiss, IEEE Trans. Magn. 38, 3365 (2002).
6. Magnetic Sensors and magnetometers (P. Ripka *et al*) ISBN: 1580530575.
7. B. Payet, D. Vincent, L. Delaunary, and G. Noyel: J. Magn. Magn. Mater. 186 (1998) 168.
8. K. Enpuku, T. Tanaka, Y. Tamai, F. Dang, N. Enomoto, J. Hojo, H. Kanzaki, and N. Usuki: Jpn. J. Appl. Phys. 47 (2008) 7859.
9. S. X. Wang and G. Li, "Advances in giant magneto resistance biosensors with magnetic nanoparticle tags: Review and outlook," *IEEE Trans. Magn.*, vol. 44, pp. 1687–1702, 2008.
10. H. B. Hong, H. J. Krause, K. B. Song, C. J. Choi, M. A. Chung, S. W. Son, and A. Offenhausser, "Detection of two different influenza A viruses using a nitrocellulose membrane and a magnetic biosensor," *J. Immunol. Meth.*, vol. 365, pp. 95–100, 2011.
11. R. Gaster, L.Xu, S. J. Han, R. J. Wilson,D.A. Hall, S. J.Osterfeld, H. Yu, andS.X.Wang, "Quantification of protein interactions and solution transport using high-density GMR sensor arrays," *Nat. Nanotechnol.*, vol. 6, pp. 314–320, 2011.

12. H. Grossman, W. Myers, V. Vreeland, R. Bruehl, M. D. Alper, C. R. Bertozzi, and J. Clarke, "Determination of bacteria in suspension using a superconducting quantum interference device," *PNAS U. S. A.*, vol. 101, pp. 129–134, 2004.
13. A. Fornara, P. Johansson, K. Petersson, S. Gustafsson, J. Qin, E. Olsson, D. Ilver, A. Krozer, M. Muhammad, and C. Johansson, "Tailored magnetic nanoparticles for direct and sensitive detection of biomolecules in biological samples," *Nano Lett.*, vol. 8, pp. 3423–3428, 2008.
14. M. Stromberg, T. Torre, J. Goransson, K. Gunnarsson, M. Nilson, P. Svedlindh, and M. Stromme, "Multiplex detection of DNA sequences using the volume-amplified magnetic nanobead detection assay," *Anal. Chem*, vol. 81, pp. 3398–3406, 2009.
15. K. Enpuku, Y. Tamai, T. Mitake, T. Yoshida, andM.Matsuo, "AC susceptibility measurement of magnetic markers in suspension for liquid phase immunoassay," *J. Appl. Phys.*, vol. 108, p. 034701, 2010.
16. M. J.Chiu, H.E. Horng, J. J. Chien, S.H. Liao,C.H.Chen, B. Y. Shih, C. C. Yang, C. L. Lee, T. F. Chen, S. Y. Yang, C. Y. Hong, and H. C.
17. Yang, "Multi-channel SQUID-based ultra-high-sensitivity in-vitro detections for bio-markers of Alzheimer's disease via immunomagnetic reduction," *IEEE Trans. Appl. Supercond.*, vol. 21, pp. 477–480, 2011.
18. A. K. Bhuiya, T. Mitake, M. Asai, T. Ito, S. Chosakabe, T. Yoshida, K. Enpuku, and A. Kandori, "Liquid-phase immunoassays using Brownian relaxation of magnetic markers," *IEEE Trans. Magn.*, vol. 47, pp. 2867–2870, 2011.
19. K. Enpuku, H. Watanabe, Y. Higuchi, T. Yoshida, H. Kuma, N. Hamasaki, M. Mitsunaga, H. Kanzaki, and A. Kandori, "Characterization of magnetic markers for liquid-phase immunoassays usingBrownian relaxation," *Jpn. J. Appl. Phys.*, vol. 51, p. 023002, 2012.
20. ***Anwarul Kabir BHUIYA***, Masaki ASAI, Takashi YOSHIDA and Keiji ENPUKU, "Magnetic Sensor Based Liquid-Phase Immunoassays for the Detection of Biological Targets". Research reports on information science and electrical engineering of Kyushu University 16(2) p45-50; 2011-09-26.